J Solid State Electrochem (2001) 5: 412–418
DOI 10.1007/s100080000165

ORIGINAL PAPER

S. Neves · C. Polo Fonseca · R.A. Zoppi
S.I. Córdoba de Torresi

Polyaniline composites: improving the electrochemical properties by template synthesis

Received: 18 April 2000 / Accepted: 26 July 2000 / Published online: 11 May 2001
© Springer-Verlag 2001

Abstract We have been exploring the idea of using the heterogeneous porosity of inorganic (sol-gel silica) and organic (poly(vinylidene fluoride)) films as a template for the preparation of polyaniline composites. The large size pore distribution (~2.5–800 nm) in both template matrices results in a part of the polyaniline growing more ordered than in films synthesized without spatial restriction. Small-angle X-ray scattering and scanning electron microscopy experiments were done to determine the extreme values of the pore diameters. Using other experimental techniques, including cyclic voltammetry, UV-Vis-NIR spectroscopy, electrochemical impedance and chronopotentiometry, we concluded that the electrochemical properties of polyaniline, such as oxidation and reduction charges, diffusion coefficient and charge-discharge capacity, are improved in these composites.

Keywords Polyaniline · Composite · Template

Introduction

Polymeric systems are a field of increased scientific and technical interest, offering the opportunity to obtain a broad variety of promising new materials, with a wide range of properties and applications. The properties of these polymers are strongly dependent on their microstructure and morphology, which are determined by their synthesis conditions [1, 2, 3, 4].

Polyaniline (PAni) is one of the most investigated and commercialized conducting polymers [5]. The great interest in this material stems from its ability to be rapidly and reversibly cycled between the conductive and insulating states, associated with good stability, facility of preparation and the low cost of the monomer [6, 7, 8]. Although much progress has been made in the understanding of its conduction mechanism, a detailed microscopic picture of the transport process has not yet been established [9]. Charge transport of PAni and other conductive polymeric films is an intricate subject since their structure and morphology are very complex. The charge transport mechanisms along a single molecule or a chain of a variety of conductive polymers are so far quite well understood. In general, the models are based on a periodic arrangement of monomers with a random distribution of defects along the backbone [10, 11]. The most important consideration from a chemical viewpoint is that better conductivity and electrochemical properties are obtained when the polymers are prepared with enhanced molecular and supermolecular order and, consequently, containing fewer conjugation-interrupting defects, such as sp^3-hybridized carbons or twists and kinks in the polymer chain [12, 13, 14].

Among the different strategies to synthesize more ordered materials reported in the literature, template synthesis is an elegant approach [15]. This technique consists of including metallic or organic constituents (guests) inside the void spaces of host materials. These void spaces act as a template that determines the shape, size and, in many cases, the orientation of the produced particle. When the host matrix is not dissolute, a composite is obtained.

There is a huge range of host materials ([16] and references therein). Since 1985, Martin and co-workers [17, 18, 19] have used commercial membranes (Nuclepore, Poretics and Whatman) as templates to prepare nanofibrils composed of metals, semiconductors

S. Neves (✉) · S.I. Córdoba de Torresi
Instituto de Química, Universidade de São Paulo,
CP 26077, 05599-970, São Paulo SP, Brazil
E-mail: sneves@usf.com.br
Tel.: +55-11-45348071
Fax: +55-11-45241933

S. Neves · C. Polo Fonseca
LCAM, Centro de Ciências Exatas e Tecnológicas,
Universidade São Francisco,
13251-900, Itatiba SP, Brazil

R.A. Zoppi
Instituto de Ciências Biológicas e Química,
Pontifícia Universidade Católica de Campinas,
13020-904, Campinas SP, Brazil

and conducting polymers. Until now, concerning the deposition of conducting polymers, most of their work has focused on the chemical synthesis of polypyrrole, polyaniline and polymethylthiophene [20].

In this work, we report the use of template synthesis to prepare conducting polymer composites by the electrochemical polymerization of aniline in the heterogeneous void spaces of inorganic (sol-gel silica) and organic (poly(vinylidene fluoride), PVDF) porous films. Composites with conjugated polymers are interesting because of the perceived potential for combining properties that are difficult to attain separately from the individual components. We analyzed the electrochemical behavior of PAni/silica and PAni/PVDF by comparing with PAni films prepared under the same conditions.

Experimental

Synthesis of sol-gel films

Stock sol-gel solutions were prepared by mixing 4.5 mL of tetraethyl orthosilicate (TEOS, Merck) with 4.5 mL of 1,1,3,3-tetramethyl-1,3-diethoxydisiloxane (TMDES, Hüls America), 9.0 mL of methanol and 0.3 mL of 0.15 mol L^{-1} HCl. The mixture was stirred at room temperature (25 °C) for about 1 h; then it was spin-coated (3000 rpm) on glass plates coated with indium-tin oxide (ITO) and dried at room temperature. This resulted in the evaporation of the methanol, leaving behind a thin sol-gel film (2.3 μm thickness).

Preparation of PVDF membranes

Solutions of PVDF (Aldrich) (8% (w/w)) in dimethylacetamide (DMA, Merck) were spin-coated (3000 rpm) at room temperature on ITO glass. Phase separation was promoted by immediate immersion in a non-solvent bath (isopropanol). The thickness of the porous film was found to be about 2.5 μm.

Template synthesis of PAni

The polymerization of PAni inside the porous films was carried out in potentiodynamic mode by cycling the potential from 0.10 to 0.80 V vs. Ag/AgCl, using a three-electrode setup. The working electrode consisted of an ITO glass coated with silica or PVDF film, while a platinum plate served as an auxiliary electrode. The electrolyte consisted of 1.0 mol L^{-1} HCl and 1.0 mol L^{-1} NaCl containing 0.1 mol L^{-1} of distilled aniline. The polyaniline mass was calculated from the deposition charge [21] ($Q_{oxidation} = 1.05$ mC cm^{-2}) and was 0.507 μg.

Synthesis of PAni

The polymerization of PAni was carried out under the same conditions described above, directly on the ITO substrate.

Electrochemical characterization

Cyclic voltammetry, electrochemical impedance spectroscopy and chronopotentiometry measurements were made in a three-electrode one-compartment cell using 1.0 mol L^{-1} HCl and 1.0 mol L^{-1} NaCl as the electrolyte. An Ag/AgCl electrode was used as the reference, the counter electrode was a Pt plate and the working electrode was an ITO plate, modified with the composite or PAni film. The voltammograms and chronopotentiometric data were obtained by an AUTOLAB-PGSTAT20 potentiostat.

Impedance spectra were recorded by a Solartron 1255 HF frequency response analyzer coupled with a PAR 273a potentiostat, both interfaced with a personal computer. An a.c. amplitude of 10 mV was applied and data were collected in the frequency range 10^{5}–10^{-2} Hz, taking 10 points per decade. The electrode potential (E) was varied in steps of 25 mV in the potential range from 0.35 to 0.65 V, which corresponds to the conducting state of polyaniline. Before each frequency sweep the electrode was prepolarized at E for about 1 h. The impedance data were analyzed by Boukamp's fitting program [22, 23].

Scanning electron microscopy

The SEM data were obtained using a JEOL JSM T-300 microscope, after coating the samples films with gold by sputtering.

UV-Vis-NIR spectroscopy

The UV-Vis-NIR measurements were carried out using a CARY 5G (Varian) spectrophotometer. The background signal emanating from native template matrix films were corrected from the UV-Vis-NIR diffuse reflectance spectra of the respective composites films.

Small-angle X-ray scattering

SAXS measurements were carried out at LNLS-Laboratório Nacional de Luz Síncrotron (Campinas, Brazil), using their synchrotron radiation facilities ($\lambda = 1.729$ Å). The raw data were corrected for decay of beam intensity, detector sensitivity, background and parasitic scattering which originated from the Mylar windows.

Results and discussion

The color of the porous films was changed from transparent (silica) and white (PVDF) to green after composite formation. This is the typical color of the half-oxidized, emeraldine form of PAni and indicates that a polymer was formed inside the void spaces of the template matrices. The scanning electron micrographs in Fig. 1 show a larger porous size distribution and strong changes in the surface morphology between the host matrices and the respective composites.

Although all films present porous morphologies, we observe an evident diminution of pore sizes in the composites as a function of PAni polymerization. Complex electrochemical processes operate during the diffusion of aniline into the template matrices, but we believe that the monomers are anchoring on the underlying ITO surface (substrate) and the polymer is preferentially deposited as thin layers on the pore wall (PVDF film) or along the walls of globular particles (silica film). This runs through the entire thickness of both template matrices and it must be noted that the polymer forms a continuous conducting network within the composite films.

Figure 2 shows the cyclic voltammograms of polyaniline film and composites in 1.0 mol L^{-1} HCl solution containing 1.0 mol L^{-1} NaCl at 5 mV s^{-1}. Cycles were repeated ca. five times to obtain a steady-state voltammogram. The voltammetric peaks correspond to the

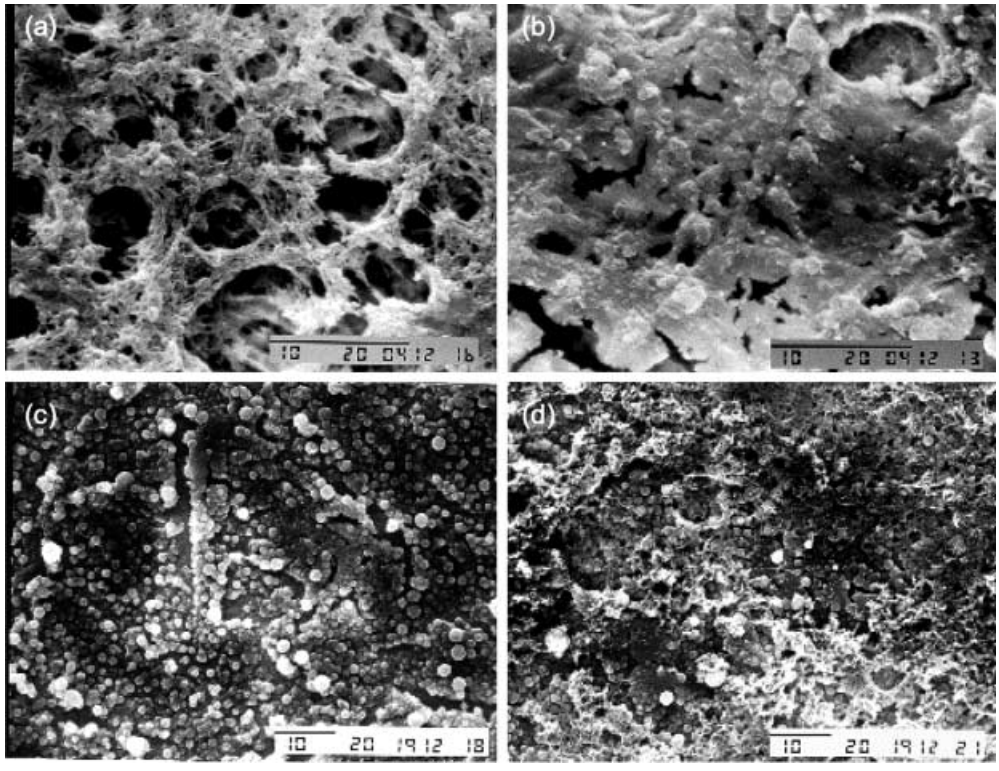

Fig. 1 Scanning electron micrographs of **a** PVDF, **b** PAni/PVDF, **c** sol-gel silica and **d** PAni/silica films

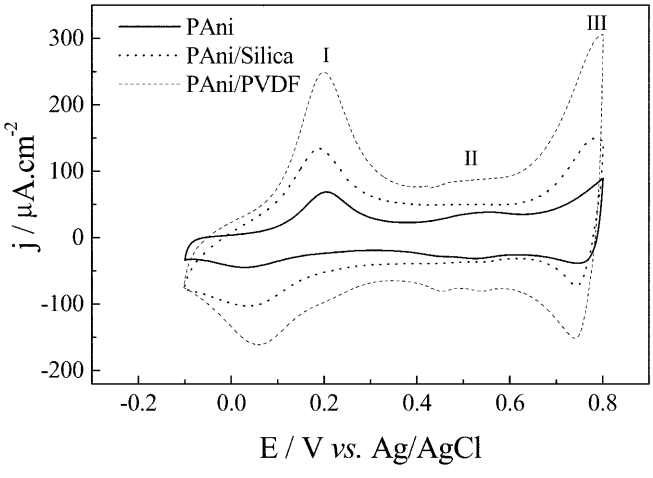

Fig. 2 Steady-state cyclic voltammograms of polyaniline film and composites in 1.0 M HCl solution containing 1.0 M NaCl at 5 mV s^{-1}

changes in the oxidation state of the polyaniline that can be related to the ratio between the amine and imine content in the film [24]. The first anodic process, which appears close to 0.2 V, is associated with the oxidation of the leucoemeraldine to emeraldine [25]; the third oxidation process (at about 0.79 V) is related to the oxidation of the emeraldine to pernigraniline. During the reverse scan, the backward reactions exhibited reversible redox processes in the potential range analyzed.

The cyclic voltammograms included an additional middle peak between the two main sets of peaks, assigned to defects in the linear polymer structure (cross-linking) [6, 26]. The cross-linking reactions give rise to an interruption in the delocalization of both the charge and electrons along the polymer chain [27]. Then, the intermediate peak can be correlated to a decrease of the conductivity and an increase in the number of residual spins in the polymer upon potential cycling [28, 29, 30]. The intermediate redox couple in the cyclic voltammogram is strong with PAni and particularly weak with PAni/PVDF films. Its absence in the PAni/silica voltammogram indicated that the spatial restraint in the sol-gel silica matrix is sufficient to induce the formation of more ordered polyaniline chains in this composite. After a large number of voltammetric cycles with PAni/silica films the redox peaks became less defined; however, there is no formation of an intermediate redox couple.

From the analysis of voltammograms we can also observe that the redox charge is more intense in the order: PAni < PAni/silica < PAni/PVDF. The film porosity increases in the same order, indicating that the swelling of the composite bulk by the electrolyte solution should be also considered. The higher bulk interaction of the film with the electrolyte solution results in the intensification of the redox processes.

Diffuse reflectance spectra of PAni and composites films (Fig. 3) show two distinct bands: one centered at ~380 nm and another at ~800 nm. According to Xia and co-workers [31], these bands can be described to the polaron-π^* transition and π-polaron transition. Note that the more significant difference between the spectra is an increasing absorption tail extended towards the NIR

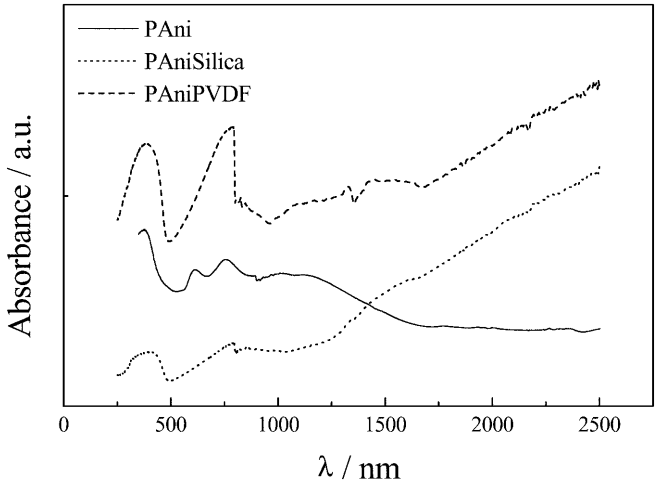

Fig. 3 UV-Vis-NIR spectra for polyaniline film and composites

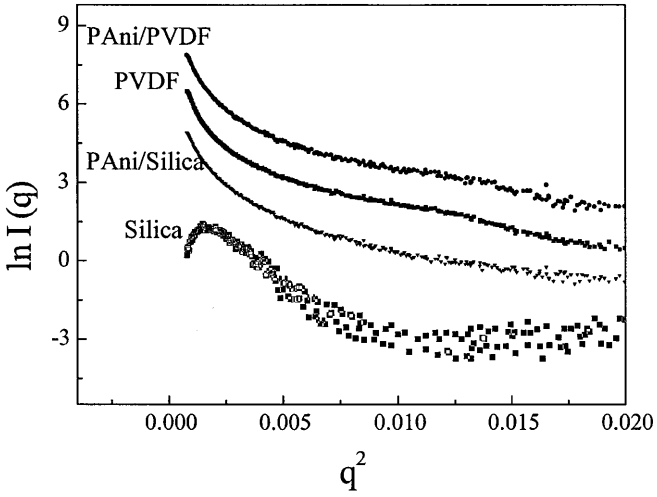

Fig. 4 Guinier region of the SAXS spectra for polyaniline film and composites

region, observed only in the composites. This extended "free carrier tail" corresponds to a decrease in the band gap, which is a direct consequence of an increase in the conjugation length [32]. Since no NIR absorption tail is observed with PAni film, it can be concluded that polarons (the dominant charge carriers in polyaniline) are more localized than in the composite films.

The different behavior observed between bulk polyaniline and its composites could be related to spatial restrictions imposed by the template matrices. Nevertheless, the pore sizes of matrices observed in the scanning electron micrographs (Fig. 1) are not sufficiently small to provide partial order in the polymer chains [33, 34]. In fact, one can suppose that a certain order can be induced by smaller pores, which are not observed in these micrographs.

To confirm this hypothesis, small-angle X-ray scattering (SAXS) measurements were performed to investigate the porosity of the template matrices. This technique is useful to investigate the structure of materials on a scale from about 0.5 to 200 nm [35]. In scattering experiments, one measures the scattered-intensity profile (I) of the sample as a function of the scattering vector, q. If a two-phase model (solid matrix and pores) is assumed, the porosity can be determined by electronic density variations [36, 37]. In the low q region, the radius of gyration R_g can be calculated and provides information about the mean size of the scattering particles (pores in our samples) and the degree of overlap and interaction between the scattering structures [38].

In Fig. 4 the Guinier plots (ln I versus q^2) are slightly concave, which can be expected for physical systems consisting of a large number of scatterers (pores of several sizes). Since in all these cases the Guinier regions are almost linear on the scale used, the radius of gyration and the size of the primary building scatter unit (r_0) can be estimated using a linear fit of the Guinier region. The results are summarized in Table 1.

Based on the results, structural information for the matrices and composite films can be envisaged as follows: the primary pore size (r_0) is defined by the smaller porosity of the template matrices and it remains the same size after the PAni synthesis, eventually contributing to a large proportion of the ultra-micropores in both matrices. The secondary pore structures (R_g), on the other hand, present a size decrease after the PAni growth but were not completely occupied in the synthesis conditions.

Table 1 Experimental microstructural parameters for template matrices and respective composites

Sample	Silica	PAni/silica	PVDF	PAni/PVDF
R_g (Å)	26	21	24	18
R_0 (Å)	6	6	8	7

These data show that template-synthesized polyanilines have more ordered polymer chains than the corresponding material obtained by conventional synthesis owing to the presence of pores with diameters ≥25 Å in the matrices.

Impedance spectroscopy was used to investigate the charge transport characteristics of polyaniline composites. This is one of the most powerful techniques that has been applied to study conducting polymer film coated electrodes [39, 40, 41, 42]. As a result of the porous nature of the electrodes and the structural changes that accompany polyaniline redox processes, separation of the faradaic and non-faradaic contributions to the current was difficult. Figure 5 shows the change of the composites impedance spectra in a potential interval between the redox peaks (I and III in voltammogram, Fig. 2), within which the electronic conductivity of PAni is high and the faradaic processes in the composite electrode are not expressive.

The impedance responses of the PAni/silica system (Fig. 5a) at all potentials consist of three distinct regions. (1) A semicircle at higher frequency related to the charge transfer process, which was electrically described

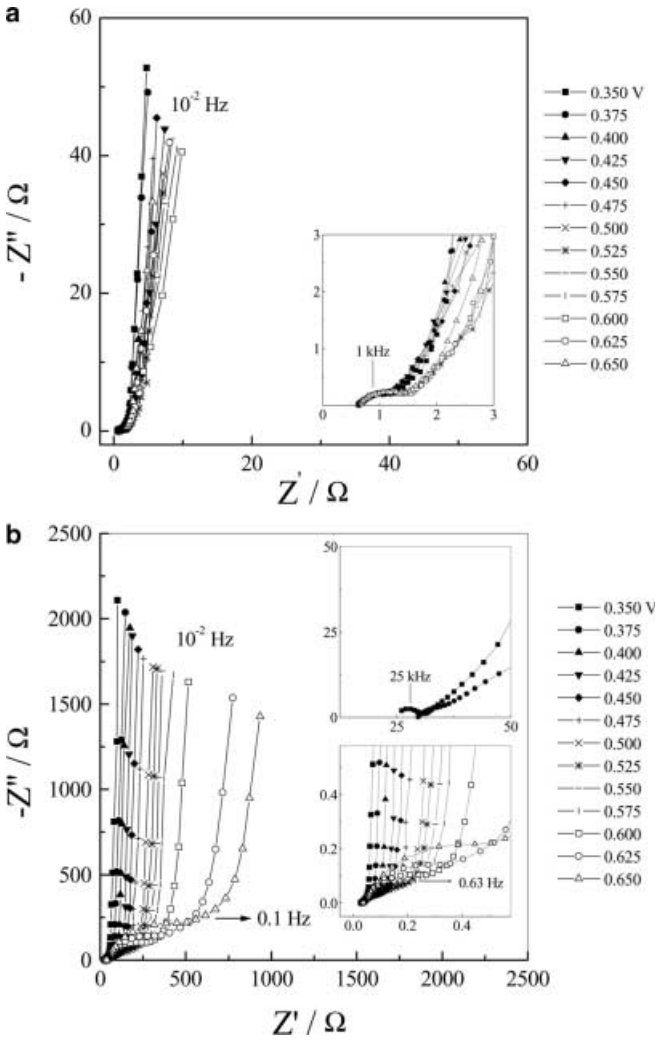

Fig. 5 Complex plane plots of successive impedance measurements of **a** PAni/silica and **b** PAni/PVDF, in the potential range between the two oxidation peaks of polyaniline ($E = 0.350$–0.650 V vs. Ag/AgCl). The electrode potential was varied in steps of 25 mV in 1.0 mol L^{-1} HCl/1.0 mol L^{-1} NaCl electrolyte

by a resistance in parallel with a capacitor related to charge transfer and a electrode/polymer double layer, respectively. It also contains contributions from the bathing electrolyte. (2) A 45° line in the complex-plane impedance plot defining a Warburg region of semi-infinite diffusion of species in the polymer. (3) At the limit of low frequencies, the impedance becomes capacitive and of magnitude. A nearly vertical line defines the region of finite diffusion that was represented electrically by a capacitor [42].

In the first and last potentials the same behavior was observed with the PAni/PVDF composite, however, in the potential range from 0.375 to 0.575 V, no high-frequency semicircle was detectable (Fig. 5b). Only diffusion-controlled characteristics were observed in this potential range, probably owing to the higher porosity of PAni/PVDF that facilitated the ionic transfer process.

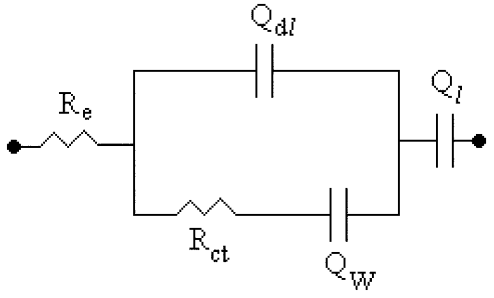

Fig. 6 Equivalent circuit for composites films, where R_e is electrolyte resistance, Q_{dl} is double-layer capacitance, Q_w is Warburg impedance, R_{ct} is charge transfer resistance and Q_l is limit capacitance

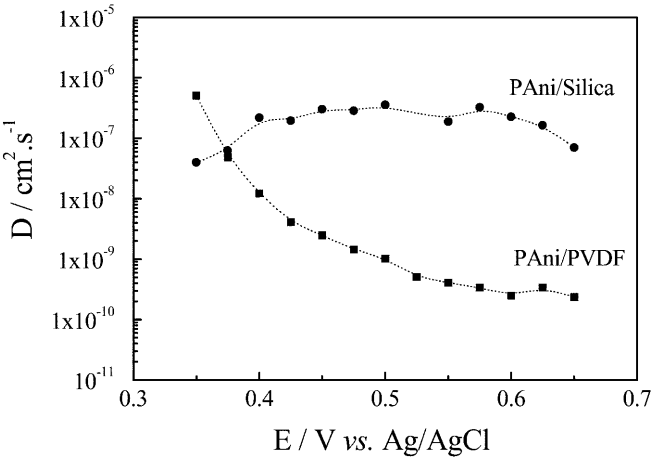

Fig. 7 Plot of diffusion coefficient as a function of applied potential

These spectra data were fitted using the non-linear least-squares fit routines [22, 23], where all parameters in the equivalent circuit model were adjusted simultaneously (Fig. 6).

In the case of the PAni/PVDF composite, the double-layer capacitance (Q_{dl}) was not determined because the ionic diffusion processes were already observed at higher frequencies.

Analysis of the Warburg and low-frequency regions of the impedance spectra resulted in values for the limit capacitance (Q_l) and diffusion coefficient (D), assuming that the electronic charge is much more mobile than the ions because the polyaniline was in its conductive form [43]. Q_l values of about 10 and 160 mF cm^{-2} correspond to the charge storage capacity of the PAni/PVDF and PAni/silica films, respectively. In the conducting potential range analyzed, the limit capacitance was nearly independent of the electrode potential for both cases.

The diffusion coefficients (Fig. 7) were calculated using the equivalent circuits show in Fig. 6 and Eq. 1 (described in [42]):

$$\tau = B^2/3 = l^2/3D \quad (1)$$

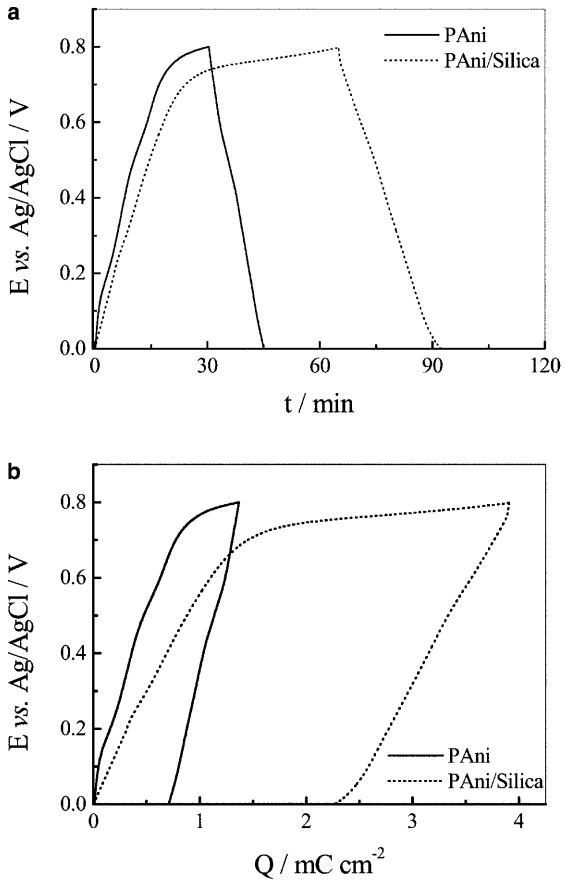

Fig. 8 **a** Chronopotentiometry and **b** charge-discharge curves of PAni film and PAni/silica composite in 1.0 M HCl solution containing 1.0 M NaCl; current density 1 μA cm^{-2}

where B is a hyperbolic function, determined by data fitting, and l is the film thickness.

It is notable in Fig. 7 that the ion diffusion process for PAni/silica is practically constant (4×10^{-8} cm^2 s^{-1}) from the 0.400 to 0.625 V potential range investigated and higher than PAni/PVDF. The PAni/PVDF diffusion values decrease when this composite is oxidized. This variation can be related to a structural change in the film that is stronger in the composite with smaller spatial restriction and therefore with the polymeric chain less ordered. In both cases the diffusion coefficients determined are higher than the values reported in the literature for electrochemical polyaniline [42].

As PAni/silica shows a high storage capacitance observed by EIS, its charge-discharge behavior was investigated through chronopotentiometric experiments (Fig. 8a, b) carried out under a constant current density (1 μA cm^{-2}). Figure 8a shows the preliminary results of the chronopotentiometric experiments, which were obtained for the second cycle. In these experiments we employed the maximum and minimum cut-off potentials of 0.8 V and 0.0 V, respectively. Taking these results, charge-discharge curves could be calculated (Fig. 8b). The charge determined for PAni/silica is significantly higher than for PAni film, 3.9 and 1.4 mC cm^{-2}, respectively. The composite delivered approximately 60% discharge capacity, while the PAni electrode showed 50%.

Conclusions

Based on these results, we conclude that it is possible to enhance the molecular order of polyaniline chains in composites by using sol-gel silica and PVDF membranes as templates. Owing to a larger pore size distribution in both template matrices, the polymer forms a continuous conducting network within the composite films, but porous morphologies are still observed. The porous structure of the composites permits a higher swelling of the polyaniline by the electrolyte solution and the formation of parallel ionic and electronic conduction paths, which also contribute to improve the electrochemical properties of these materials. Their use in devices for charge storage is now under investigation, for a better understanding of the synthesis-structure-properties relationships in these composites.

Acknowledgements The authors thank FAPESP (proc. 97/03395-1 and 96/6942-0) for financial support, National Synchrotron Light Laboratory, Brazil, and Prof. Iris Torriani from IFGW, Unicamp, for the measurements and valuable discussions related to the SAXS experiments.

References

1. Cordova R, del Valle MA, Aratia A, Gomez R, Schrebler R (1994) J Electroanal Chem 377:75
2. Koziel K, Lapkowski M (1993) Synth Met 55–57:1011
3. Andrade GT, Aguirre MJ, Biaggio SR (1998) Electrochim Acta 44:633
4. Inzelt G, Horanyi G (1989) J Electrochem Soc 136:1747
5. Trivedi DC (1997) In: Nalwa HS (ed) Handbook of organic conductive molecules and polymers, vol 2. Wiley, Chichester, UK, pp
6. Geniès EM, Boyle A, Lapkowski M, Tsintavis C (1990) Synth Met 36:139
7. Yoneyama H, Wakamoto K, Tamura H (1985) J Electrochem Soc 132:2414
8. Thackeray JW, White HS, Wrighton MS (1985) J Phys Chem 89:5133
9. Bredas JL, Street GB (1985) Acc Chem Res 18:309
10. Heeger AJ, Kivelson S, Schrieffer JR, Su WP (1988) Rev Mod Phys 60:781
11. Kivelson S, Heeger AJ (1988) Synth Met 22:371
12. Fosong W, Jinsong T, Lixiang W, Hongfang Z, Zhishen M (1988) Mol Cryst Liq Cryst 160:175
13. Lei J, Cai Z, Martin CR (1992) Synth Met 46:53
14. MacDiarmid A (1993) In: Salaneck WR, Lundstrom I, Ranby B (eds) Conjugated polymers and related materials. Oxford University Press, Oxford, pp
15. Ozin GA (1992) Adv Mater 4:612
16. Farrington G, Shriver DF (1985) Chem Eng News 63:42
17. Penner RM, Martin CR (1986) J Electrochem Soc 133:2206
18. Martin CR (1996) Chem Mater 8:1739
19. Hulteen JC, Martin CR (1997) J Mater Chem 7:1075
20. Martin CR (1995) Acc Chem Res 28:61
21. Koryta J, Dvorák J, Kavan L (1993) Principles of electrochemistry, 2nd edn. Wiley, Chichester, UK, pp
22. Boukamp BA (1986) Solid State Ionics 20:31

23. Boukamp BA (1989) Equivalent circuit. University of Twente, The Netherlands
24. Snauwaert P, Lazzaroni R, Riga J, Verbist J, Gonbeau D (1989) Electronic properties of conjugated polymers III, vol 91. Springer, Berlin Heidelberg New York, pp 301–304
25. Huang W, Humphrey BD, MacDiarmid AG (1986) J Chem Soc Faraday Trans I 82:2385
26. Karyakin AA, Maltsev IA, Lukachova LV (1996) J Electroanal Chem 402:217
27. Geniès EM, Lapkowski M, Penneau JF (1988) J Electroanal Chem 249:97
28. Epstein AJ, Ginder JM, Zuo F, Bigelow RW, Woo HS (1987) Synth Met 18:303
29. Geniès EM, Lapkowski M (1987) J Electroanal Chem 236:199
30. Glarum SH, Marshall JM (1987) J Electroanal Chem 134:2160
31. Xia Y, Wiesinger JM, MacDiarmid AG, Epstein AJ (1995) Chem Mater 7:443
32. Zagorska M, Pron A, Lefrant S (1997) In: Nalwa HS (ed) Handbook of organic conductive molecules and polymers, vol 3. Wiley, Chichester, UK, pp
33. Martin CR, Parthasarathy R, Menon V (1993) Synth Met 55–57:1165
34. Wu CG, Bein T (1994) Science 264:1757
35. Wong PZ, Bray AJ (1988) J Appl Crystallogr 21:786
36. Lours T, Zarzycki J, Craievich AF, Aegerter MA, dos Santos DI (1988) J Non-Cryst Solids 106:157
37. Lours T, Zarzycki J, Craievich AF, Aegerter MA (1990) J Non-Cryst Solids 121:216
38. Boukari H, Lin JS, Harris MT (1997) Chem Mater 9:2376
39. Vorotyntsev MA, Daikhin LI, Levi MD (1994) J Electroanal Chem 364:37
40. Ferloni P, Mastragostino M, Meneghello L (1996) Electrochim Acta 41:27
41. Roβberg K, Paasch G, Dunsch L, Ludwig S (1998) J Electroanal Chem 443:49
42. Skinner NG, Hall EAH (1994) Synth Met 63:133
43. Johnson BW, Read DC, Christensen P, Hamnett A, Armstrong RD (1994) J Electroanal Chem 364:103